Meas. Sci. Technol. **19** (2008) 034023 (7pp) doi:10.1088/0957-0233/19/3/034023

MACS—a new high intensity cold neutron spectrometer at NIST

J A Rodriguez[1,3], D M Adler[3], P C Brand[3], C Broholm[2,3], J C Cook[3], C Brocker[3], R Hammond[2], Z Huang[3], P Hundertmark[3], J W Lynn[3], N C Maliszewskyj[3], J Moyer[3], J Orndorff[2], D Pierce[3], T D Pike[3], G Scharfstein[2], S A Smee[2] and R Vilaseca[3]

[1] Department of Materials Science and Engineering, University of Maryland, College Park, MD, USA
[2] Department of Physics and Astronomy, The Johns Hopkins University, Baltimore, MD 21218, USA
[3] NIST Center for Neutron Research, Gaithersburg, MD 20899, USA

Received 20 July 2007, in final form 30 November 2007
Published 30 January 2008
Online at stacks.iop.org/MST/19/034023

Abstract
We describe a novel cold neutron spectrometer under development at NIST optimized for wave vector resolved spectroscopy with incident energies between 2.1 meV and 20 meV and energy resolution from 0.05 meV ($E_i = 2.1$ meV) to 3.0 meV ($E_i = 20$ meV). By using a 1428 cm^2 double focusing PG (0 0 2) monochromator close to the National Institute of Standards and Technology (NIST) cold neutron source the instrument provides up to 5×10^8 neutrons cm^{-2} s^{-1} on a 8 cm^2 sample area. The measured performance is consistent with Monte Carlo simulations. The monochromating system, which includes radial collimators, three filters and a variable beam aperture, offers considerable flexibility in optimizing Q-resolution, energy resolution and intensity. The detector system will consist of an array of 20 channels which combined will subtend a solid angle of 0.2 sr. This is approximately a factor of 40 more than a conventional triple axis spectrometer. Each detector channel contains a vertically focusing double crystal analyzer system (DXAL) actuated by a single stepping motor. We find identical integrated reflectivity at approximately 10% coarser energy resolution for the 130′ mosaic double bounce analyzer as compared to a conventional 25′ analyzer at the same energy. The vertical focusing of the DXAL allows for smaller detectors for enhanced signal to noise with 8° vertical acceptance. Options for post sample collimators and filters provide flexibility in the choice of scattered beam energy and wavevector resolution.

Keywords: neutron instrumentation, neutron diffraction, neutron spectrometer, neutron scattering

(Some figures in this article are in colour only in the electronic version)

1. Introduction

Increasing signal count rate dramatically improves the utility of inelastic neutron scattering as a tool to probe dynamic properties of condensed matter. There are basically two ways to accomplish this (1) more flux on sample and (2) detect a greater fraction of the neutrons scattered from the sample. Here we report the development of an instrument at the NIST Center for Neutron Research that seeks greater efficiency in both ways. (1) The neutron flux on sample is enhanced using a double focusing monochromator subtending up to 6 sr to the cold neutron source [1], and (2), an array of 20 energy analyzing detector channels subtend a solid angle up to 0.1 sr to the sample. In this paper, we describe the principles behind and the overall design of the multi axis crystal spectrometer (MACS). Measurements and simulations assessing the performance of the main components, including the absolute flux on sample and the efficiency and resolution of a detector channel are also presented.

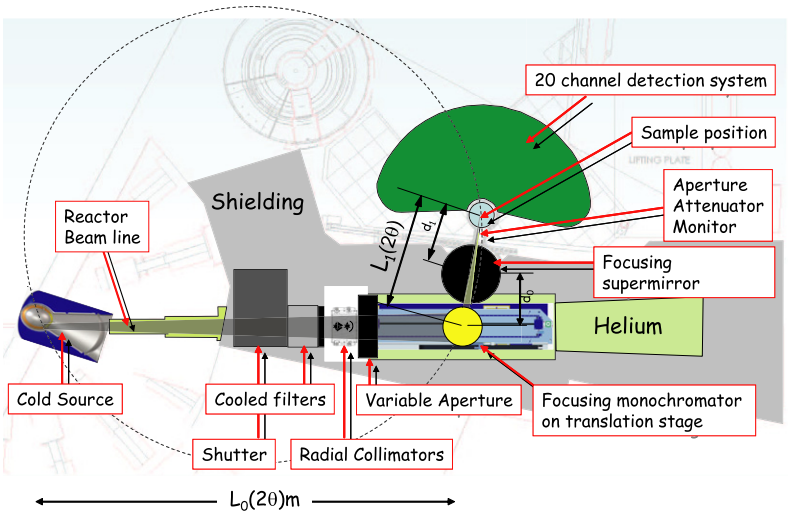

Figure 1. Schematic top view of MACS. The dashed circle which passes through the center of the source, the monochromator and the sample is named the Rowland circle after Professor Henry A Rowland, the founder of the Department of Physics and Astronomy at the Johns Hopkins University. Horizontal monochromatic focusing requires that the monochromator is tangent to the Rowland circle. The monochromating system includes two radial collimators, three filters, and a variable beam aperture for optimization of Q-resolution, energy resolution and intensity. Note that the monochromator can translate along the neutron beam from the reactor while the black monochromatic beam transport (MBT) drum rotates for beam extraction. By moving the sample around the MBT drum rather than around the monochromator as on a conventional instrument, the space required to accommodate motion of the very large detector system is reduced.

2. Instrument description

A schematic of the MACS instrument is shown in figure 1. The neutronic input is a diverging filtered cold neutron beam with a circular cross section. The rotating beam shutter has three aperture options and is placed on the experimental floor immediately outside the biological shielding. This enables extraction of the full beam cross section from the source. The cryo-filter exchanger, located downstream of the shutter, presently consists of a fixed Be filter cooled to 77 K. Eventually this system will allow cooled beryllium, graphite and most likely MgF_2 filters to be positioned between the beam shutter and the monochromating system. Two radial collimators A and B, that limit horizontal beam divergence incident on any volume element of the monochromator, can be placed after the filter. This provides four different collimation settings: open A, B and A+B which limits the horizontal divergence of radiation incident on a volume element of the monochromator to 60′, 40′ and 24′, respectively. Radially focused to the source, these collimators effectively function as source apertures to control the incident beam energy resolution.

A vertical and horizontal beam aperture can be varied automatically from closed to a 35 cm by 35 cm square. By defining the overall envelope of the beam in the horizontal and vertical planes, this aperture determines the transverse to $\mathbf{k}_i$ wave vector resolution. The doubly focusing monochromator (DFM) was designed to minimize structural materials in the neutron beam in order to reduce background [2, 3]. The DFM consists of an array of 357 pyrolitic graphite (PG) crystals attached to thin aluminum blades that can be bent and rotated to control vertical and horizontal focusing, respectively. To increase the range of incident energies while limiting the motion of the large detector system, the monochromator is moved along the reactor beamline to access different energies (see figure 1). There is no neutron guide between the cold source and the monochromator. All the components described above except the cryo-filter exchanger are already installed at the NIST Center for Neutron Research.

The monochromatic beam reaches the sample via a converging channel and beamline shielding system, named, the monochromatic beam transport system (MBT). At present the channel has fixed dimensions and is lined by ^{10}B:Al. In the future, the beam channel will be lined by a super mirror guide and the horizontal dimensions will be variable so the beam profile can be optimized. This trumpet shaped guide should increase the flux, by further broadening the transverse wave vector resolution [4]. Immediately before the sample position there will be vertical and horizontal beam slits to further crop the beam so only the sample is illuminated. There will also be single crystalline LiF attenuators with absorption factors of 1/10 and 1/100 respectively, which can be introduced into the beam under computer control. The sample table contains no magnetizable materials within 75 cm of the sample position and can support sample environment systems weighing up to 400 kg.

The detection system (figure 2) will consist of 20 identical channels surrounding the sample and separated by 8° in the horizontal scattering plane. Each channel is defined by a cast structure formed from B_4C in polyurethane. Four different collimation settings, 60′, 90′ and 36′, and open, will be available for each channel using two (60′ and 90′) conventional Soller collimators. Each channel will include three different filters (Be, BeO and graphite) cooled to less than 77 K to reduce transmission losses from inelastic scattering. Each channel will contain a vertically focusing double crystal analyzer (DXAL) (figure 3). Each of the two analyzer blades

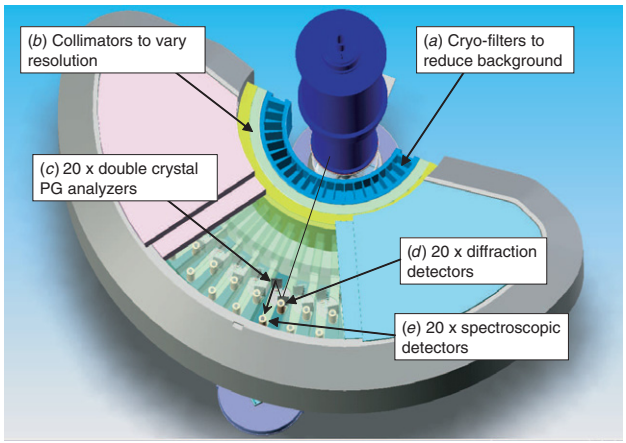

Figure 2. The detection system consists of 20 identical channels separated by 8° for a total 152° range of coverage in one setting. Each channel contains: (a) cooled Be, BeO or PG filter (b) 36′-60′-90′ or open collimation. (c) Double crystal analyzer (d) diffraction detector (e) spectroscopic detector.

consists of nine PG (0 0 2) crystals with dimensions 6.0 cm wide, 2.0 cm tall and 0.2 cm thick, mounted to form the surface of a cylinder with radius 50 cm. These can be rotated about the center of mass of the reflecting graphite. Based on a system developed for use as an x-ray monochromator [5], the DXAL mechanism both rotates and translates the two analyzer blades to transmit energies between 2.5 meV and 20 meV. This motion is actuated by a single stepping motor per DXAL and all alignment is achieved mechanically. The distance from the sample to the DXAL rotation axis is 100.0 cm and the perpendicular distance between the two analyzer translation stages within one DXAL is 7.00 cm. There will be two detectors in each of the 20 channels. The so-called diffraction detector that views the sample directly is placed behind the first analyzer. The spectroscopic detector views the second analyzer blade and so only detects neutrons that satisfy the DXAL Bragg condition. When MACS is completed, it will be possible to set different final energies for each analyzer, take **Q** area scans for a common final energy or operate the instrument as a virtual triple axis spectrometer focusing on the signal in a single channel of interest, employing always the most convenient channel for the desired scattering angle. The variable, reflective MBT, the detection system, and the presample optics are under construction at the time of writing.

3. Monte Carlo simulation

Monte Carlo simulations of the MACS incident beamline were carried out using the McStas program [6, 7] and compared to flux and resolution measurements. The McStas model of MACS provides a planning and diagnostic tool for operating and maintaining the instrument. All incident beamline components from source to the sample position were simulated, excluding only the filters. The cold source was modeled as an elliptical disk normal to the beam axis with a horizontal major axis of 20 cm and a vertical minor axis of 15 cm. The energy dependent NCNR cold source brightness was previously determined using the Monte Carlo *N*-particle transport code (MCNP) developed at Los Alamos National Labs [8] and it is shown for reference in figure 4. The beam tube between the source and monochromator was described as a series of five impenetrable apertures with circular cross sections. As described in section 2, the monochromator consists of 21 blades that can rotate and bend to control horizontal and vertical focusing, respectively. The simulation fully implements the monochromator geometry including its motion along the incident beamline.

Following [1], we define L_0 as the distance from the source to the monochromator and L_1 as the distance between the monochromator and the sample. Further denote by $d_0 = 775$ mm the perpendicular distance from the MBT center to the reactor beamline and by $d_1 = 900$ mm the fixed distance from the MBT to the sample center (see figure 1). For MACS both L_0 and L_1 vary with the monochromator scattering angle, 2θ:

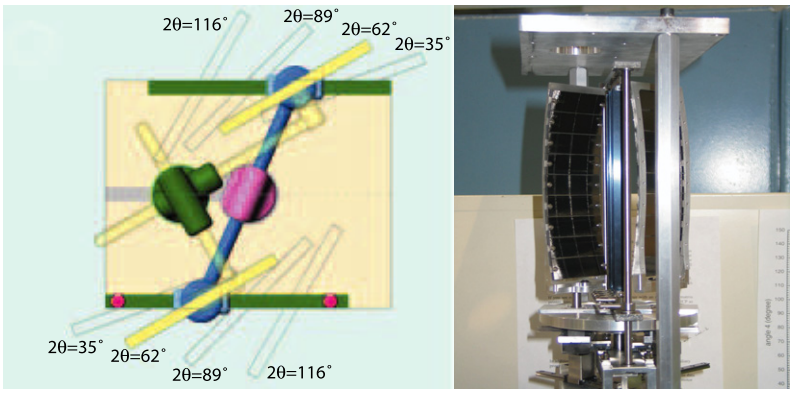

Figure 3. The vertically focusing double crystal analyzer (DXAL). The DXAL contains two vertically focusing crystals which are driven by one stepping motor. The left figure shows the mechanical linkage which assures that the two vertically focusing crystal assemblies are parallel for any angular setting so neutrons can propagate through the system via two Bragg reflections. The DXAL can transmit neutrons from 2.5 meV to 20 meV.

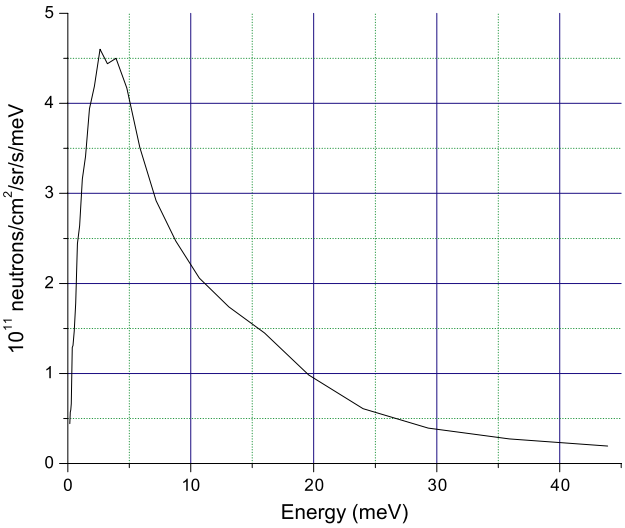

Figure 4. Cold source brightness. The cold source intensity was calculated using Monte Carlo *N*-particle transport code (MCNP) [8].

$$L_0(2\theta) = L_0(2\theta = 90^\circ) - d_0/\tan 2\theta, \tag{1}$$

and

$$L_1(2\theta) = d_1 + d_0/\sin 2\theta. \tag{2}$$

Here $L_0(2\theta = 90^\circ) = 6200$ mm. The vertical radius of curvature for the monochromator, R_v, is given by [1]:

$$R_v = \frac{2L_0L_1 \sin\theta}{L_0 + L_1}. \tag{3}$$

For Rowland focusing [1] the DFM rotation with respect to the reactor beamline is given by

$$\tan\xi = \frac{L_0 \sin 2\theta}{L_0 \cos 2\theta + L_1}. \tag{4}$$

For optimal monochromaticity blade i which is located at a distance ρ_i from the DFM center is rotated by Ψ_i with respect to the flat configuration where Ψ_i satisfies:

$$\tan\Psi_i = \frac{L_0}{L_0 \cot\xi - \rho_i/\sin\xi}. \tag{5}$$

The PG reflectivity was modeled by [9, 10],

$$\mathcal{R}_{\max} = \frac{\sqrt{2}g\,Q_h t}{1 + \sqrt{2}g\,Q_h t}, \tag{6}$$

where $g = 1/(2\sqrt{\pi}\eta)$ and $t = d/\sin(\theta)$ for a plane slab. η is the mosaic spread, d is the slab thickness, and

$$Q_h = \frac{\lambda^3 F_h^2}{v_0^2 \sin(2\theta)}. \tag{7}$$

Here v_0 is the unit cell volume, λ the wavelength and F_h is the nuclear structure factor. Two apertures defined the beam channel between the monochromator and sample. To monitor the flux on sample, a virtual detector was placed at the sample position. To optimize the focusing conditions we measured the flux on sample while varying the parameters $L_0(2\theta = 90^\circ)$ and d_1 from which the focusing conditions of the DFM are calculated. When these parameters change, the vertical radius of curvature R_v (equation (3)), the DFM array rotation ξ (equation (4)), and the individual blade rotations Ψ_i thus modify the overall imaging characteristics of the monochromating system. While the actual physical distance

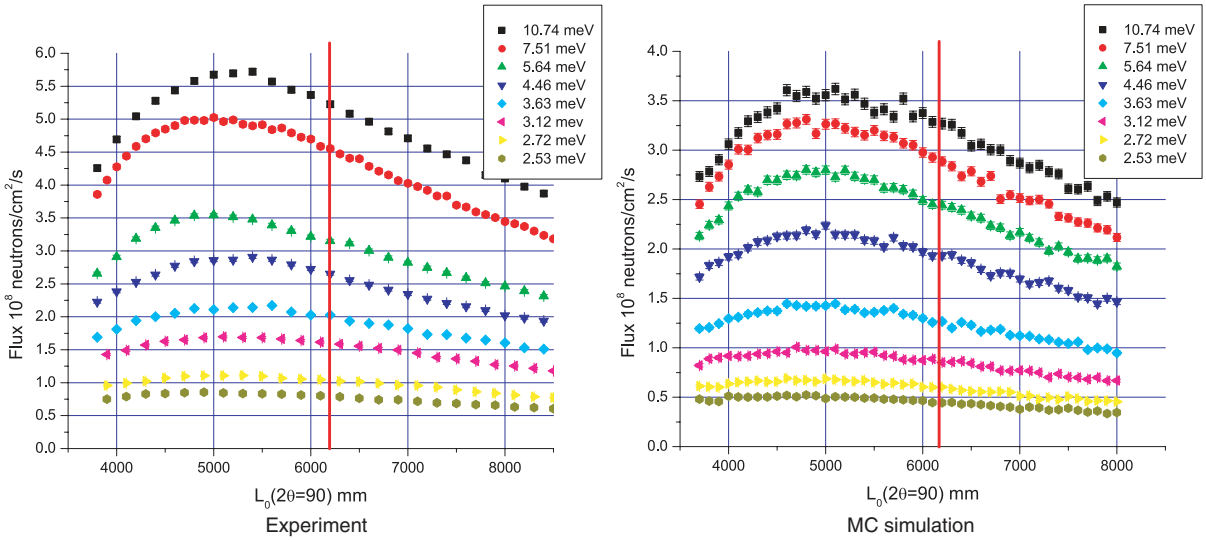

Figure 5. Measured and simulated flux on sample as a function of changes to the value of $L_0(2\theta = 90^\circ)$ used to calculate the monochromator focusing condition. $L_0(2\theta = 90^\circ)$ is the effective distance from the monochromator in reference position $(2\Theta = 90^\circ)$ to the source. Greater flux on sample is obtained with a shorter distance than the actual physical distance of 6200 mm indicated by the red lines. This indicates an effective source location in front of the actual source. The left image shows experimental data. The right image shows Monte Carlo data for the average flux on a 2 cm by 4 cm sample versus the $L_0(2\theta = 90^\circ)$ parameter used to determine the monochromator blade setting. The error bars represent one standard deviation.

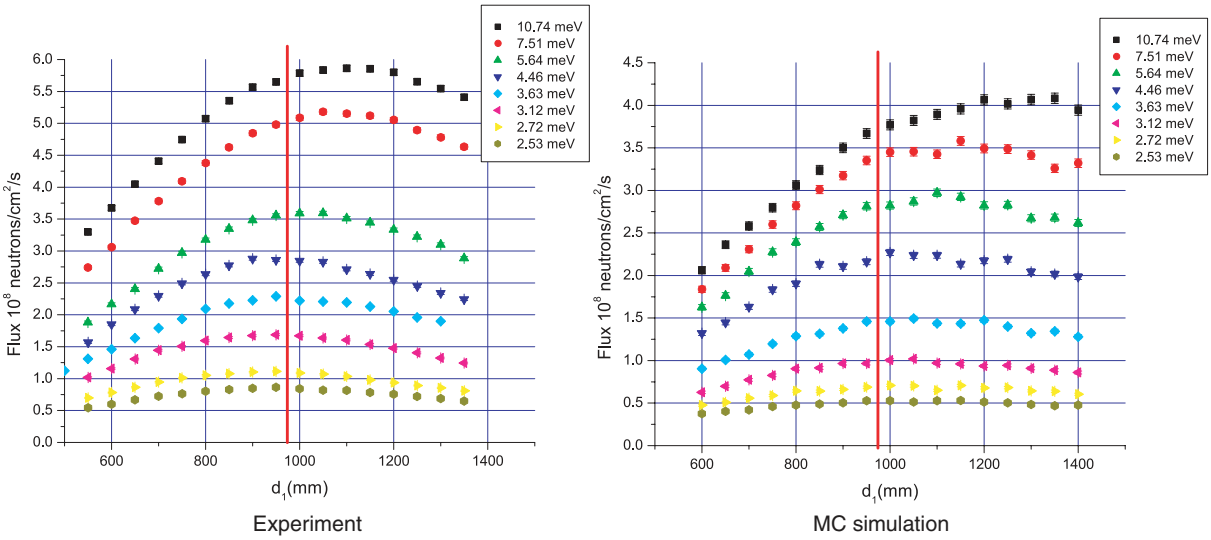

Figure 6. Measured and simulated average flux on sample versus the parameter d_1 that enters into determining the focusing setting of the monochromator through equations (2)–(5). d_1 is the nominal distance from the center of the MBT drum (black cylinder in figure 1) to the reactor beamline. The deviation of this parameter from the actual physical distance (red line) indicates that variation of it compensates for an aberration in the Bragg imaging system. The error bars represent one standard deviation.

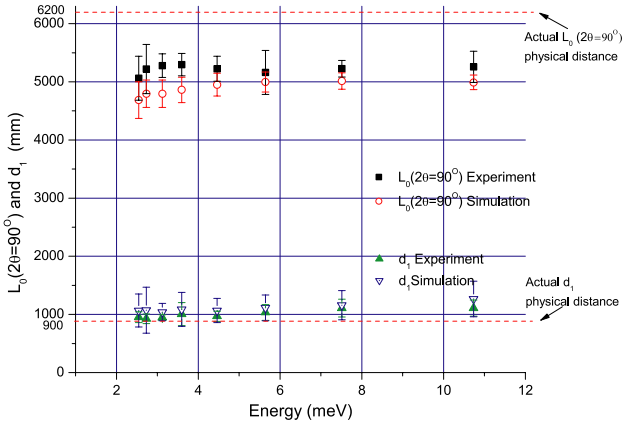

Figure 7. Energy dependence of the focusing parameters $L_0(2\theta = 90^\circ)$ and d_1 versus energy. The dashed lines show the actual physical distances. The deviations indicate optimization that accommodates aberrations between the simplified focusing calculation that is used to determine the monochromator setting and the more complicated physical reality of the instrument that compensates for aberrations. Nominally, $L_0(2\theta = 90^\circ)$ is the reference position distance from source to monochromator and d_1 is the perpendicular distance from reactor beamline to the center of the MBT drum. To extract the optimal value of $L_0(2\theta = 90^\circ)$ and d_1 the corresponding scans were fitted to a third-order polynomial. The error bars represent one standard deviation.

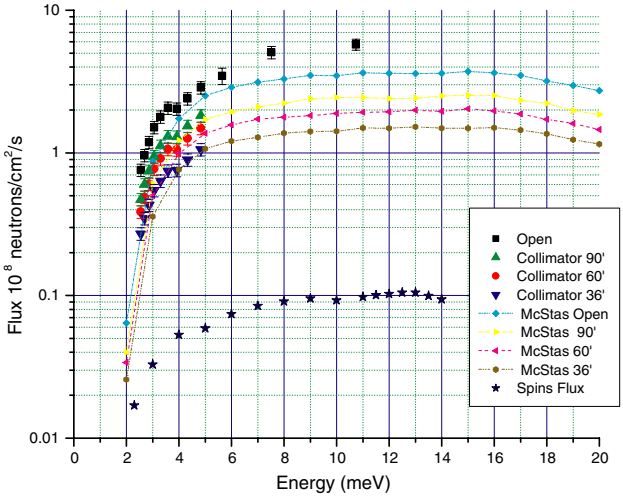

Figure 8. MACS average flux on a 2 cm by 4 cm sample versus energy. For energies below 5 meV the measurements were carried out with a Be filter in front of the source. For energies greater than 5 meV no filter was employed and the results were therefore corrected for higher order contamination using the correction factor shown in figure 9.

to the source is well known and corresponds to $L_0(2\theta = 90^\circ) = 6200$ mm, this optimization led to a 30% increase in flux on sample. A similar effect was observed in the Monte Carlo simulations (see figures 5 and 6) and this indicates that the collective adjustments are compensating for aberrations in the imaging system that are not included in the derivations leading to equations (1)–(5).

4. Beam characterization

We now describe measurements on the MACS instrument that characterize the incident beam. We placed a fission beam monitor at the sample position, and defined the typical sample dimensions by a 2 cm wide by 4 cm tall ^{6}LiF doped polymer mask. For each setting of the incident energy the monitor count rate was maximized by varying the $L_0(2\theta = 90^\circ)$ and d_1 parameters that go into calculating the monochromator

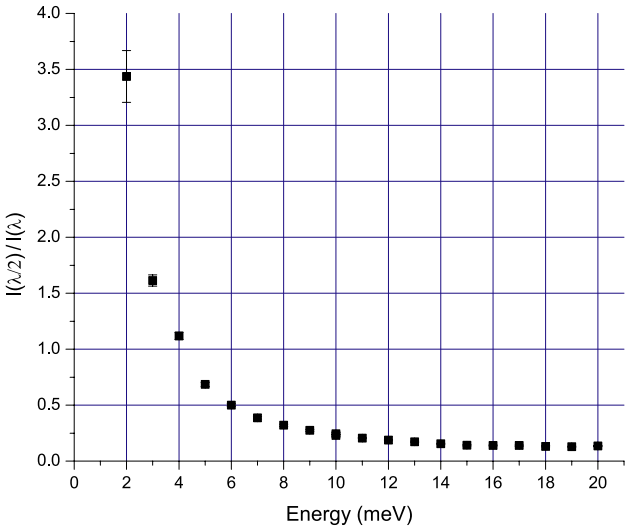

Figure 9. MACS $\lambda/2$ contribution calculated using Monte Carlo simulations. The $\lambda/2$ reflectivity was calculated using equation (6). The error bars represent one standard deviation.

focusing condition. The curves were fitted using a third-degree polynomial function to extract the optimal values of these parameters at each energy setting. The energy dependence of the optimal focusing parameters, which is in fact quite negligible, is shown in figure 7. The maximum flux versus energy is given in figure 8. The absolute flux on sample was determined using a calibrated U-235 fission chamber placed on the sample position. Above 5 meV, the instrument was operated without a filter in the incident beam and the resulting intensity measurements were corrected for $\lambda/2$. The correction factor was determined through Monte Carlo simulations and it is shown as a function of energy in figure 9. While the simulation reproduces all features of the experimental data, it actually underestimates the flux on sample by approximately 35%. This is a welcome surprise since the simulation specifically neglects a number of loss mechanisms. A likley explanation is limitations in the fidelity of the source model used in this simulation.

5. DXAL performance

An experiment was performed on the spin-polarized triple-axis spectrometer (SPINS) at the NIST Center for Neutron Research to determine the double crystal analyzer performance. SPINS has a PG (0 0 2) vertically focusing monochromator with a mosaic of 30′. The spectrometer can access energies from 2.3 meV to 14.0 meV with resolution from 0.05 meV ($E_i = 2.3$ meV) to 1 meV ($E_i = 14.0$ meV). The detector system features a 30′ mosaic PG (0 0 2) analyzer which can be horizontally focused but is not vertically focusing.

One MACS detector channel, including a DXAL, shielding and collimators, was temporarily attached to the SPINS sample table as a second detector option. The SPINS detector system with the analyzer in the non-focusing mode served as a reference. A vanadium cylinder was placed on the sample position to measure the energy resolution through incoherent elastic scattering and compare the integrated intensity for the four collimation options (90′, 60′, 36′ and open). The results are shown in figures 10 and 11. The integrated intensity for the DXAL and SPINS detectors are similar though it appears that multiple scattering effects, which modulate the reflectivity versus energy, are more prominent for the DXAL. This may be a result of the coarser mosaic (84′ as opposed to 30′) and the fact that passage through the system involves two reflections. The energy resolution for the DXAL is coarser than for the SPINS analyzer due to the coarser mosaic. To match the resolution of the DFM the DXAL mosaic was chosen to be $\sqrt{2}$ times coarser than the 60′ mosaic of the monochromator. These choices increase signal count rate at fixed energy resolution, but in general will require

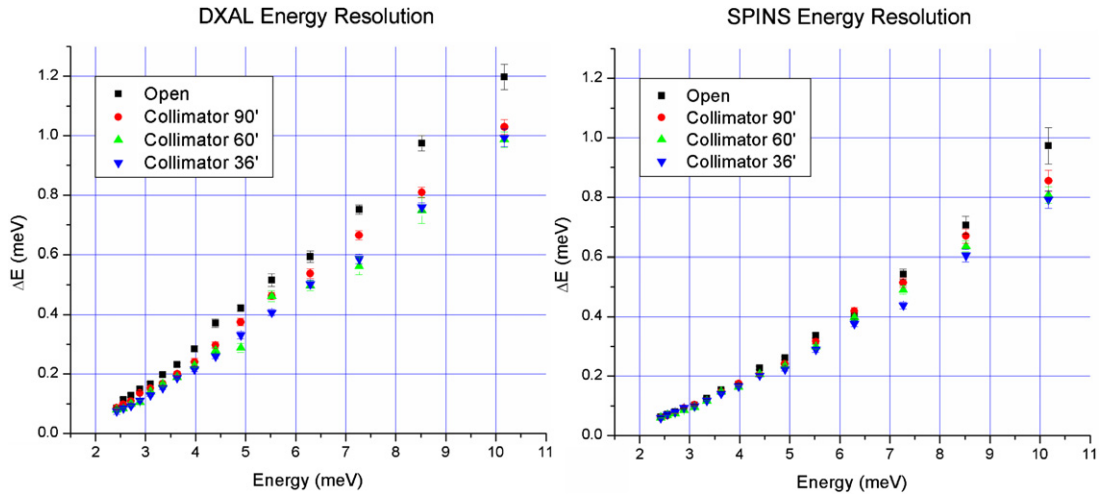

Figure 10. DXAL and SPINS energy resolution comparison graphs (90′ for collimator A, 60′ for collimator B, 36′ for collimators A+B and no collimators). The error bars represent one standard deviation.

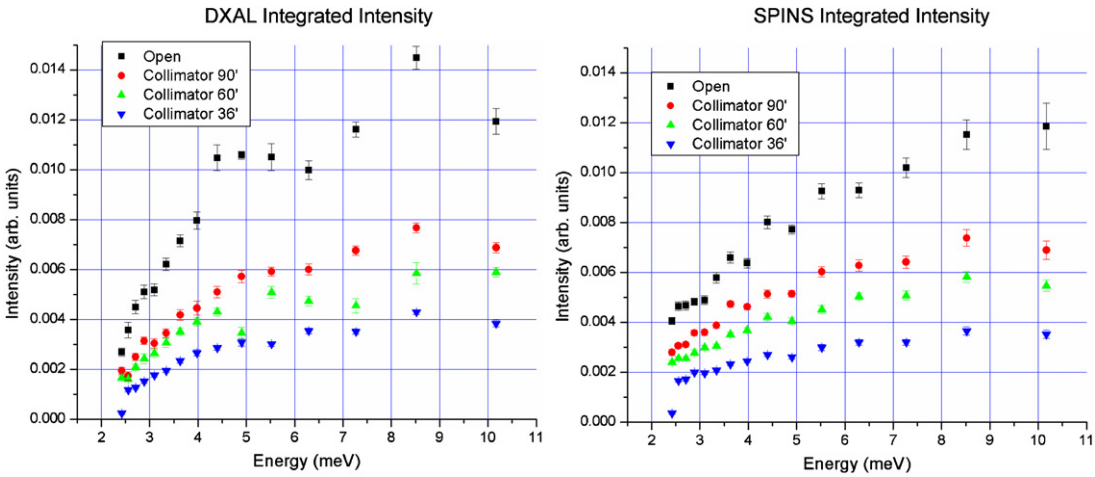

Figure 11. DXAL and SPINS analyzer integrated intensity comparison. The integrated intensity is similar for both SPINS and the DXAL. Multiple scattering effects are more prominent on the DXAL due to the different blades of the double crystal analyzer. The data demonstrate comparable performance for these systems. The error bars represent one standard deviation.

the use of lower incident energy than for a conventional 30′ mosaic PG (0 0 2) instrument.

6. Conclusions

The beam characterization experiments reported in this paper show that MACS will be one of the world's most intense cold neutron spectrometers. Indeed the flux on sample is 40 times the intensity of the existing cold neutron spectrometer, SPINS, at NIST. The MACS gains result from full illumination of a large doubly focusing monochromator. Additional performance enhancements will come from the multi-channel detector system, which subtends a solid angle of 0.1 sr to the sample. For experiments where relaxed transverse wave vector resolution can be employed and all spectroscopic detectors can be utilized, MACS should exceed the efficiency of SPINS by more than two orders of magnitude. The increased performance should allow inelastic neutron scattering to be applied to problems in material science that involve small samples or weak scattering cross sections, as well as to problems that require extensive mapping of the scattering cross section versus **Q**, ω, or thermodynamic variables.

Acknowledgments

It is a pleasure to acknowledge helpful discussions with and unwavering support from J M Rowe and J J Rush throughout the project. We also thank Steven Patterson and Scott Spangler at the Johns Hopkins University and George Baltic and his team at the NIST Center for Neutron Research for their ongoing expert technical assistance. The MACS project was supported by the US National Science Foundation under DMR-0116585.

References

[1] Broholm C 1996 Proposal for a doubly focusing cold neutron spectrometer at NIST *Nucl. Instrum. Methods Phys. Res.* A **369** 169

[2] Smee S A, Orndorff J D, Scharfstein G A, Qui Y, Brand P C, Broholm C L and Anand D K 2002 MACS low background doubly focusing neutron monochromator *Appl. Phys.* A **75** 1

[3] Smee S A, Brand P C, Barry D D, Broholm C L and Anand D K 2001 An elastic, low background vertical focusing element for a doubly focusing neutron monochromator *Nucl. Instrum. Methods Phys. Res.* A **446** 513

[4] Wildes A R, Šaroun J, Farhi E Anderson I, Høghøj P and Brochier A 2000 A comparison of Monte-Carlo simulations using RESTRAX and McSTAS with experiment on IN14 *Physica* B **276–278** 177

[5] Golovchenko J A, Levesque R A and Cowan P L 1981 X-ray monochromator system for use with synchrotron radiation sources *Rev. Sci. Instrum.* **52** 509

[6] Lefmann K and Nielsen K 1999 McStas, a general software package for neutron ray-tracing simulations *Neutron News* **10** 20

[7] Andersen P, Lefmann K, Thiel Kuhn L, Willendrup P K and Farhi E 2004 Monte Carlo simulations as a part of the configuration for neutron instruments *Physica* B **350** 735

[8] Monte Carlo *N*-Particle Program (MCNP) supported by Los Alamos National Labs http://mcnp-green.lanl.gov

[9] Bacon G E and Lowde R D 1948 Secondary extinction and neutron crystallography *Acta Cryst.* **1** 303

[10] Sears V F 1989 *Neutron Optics. An Introduction to the Theory of Neutron Optical Phenomena and Their Applications.* (Oxford: Oxford University Press)